ЯДЕРНА ФІЗИКА
NUCLEAR PHYSICS

УДК 539.171+539.172 https://doi.org/10.15407/jnpae2022.01.012

S. Yu. Mezhevych[1,*], A. T. Rudchik[1], K. Rusek[2], K. W. Kemper[3], A. A. Rudchik[1], O. A. Ponkratenko[1], E. I. Koshchy[4]

[1] *Institute for Nuclear Research, National Academy of Sciences of Ukraine, Kyiv, Ukraine*
[2] *Heavy Ion Laboratory of Warsaw University, Warsaw, Poland*
[3] *Physics Department, Florida State University, Tallahassee, USA*
[4] *Cyclotron Institute Texas A&M University, College Station, USA*

*Corresponding author: sermezhev@gmail.com

REACTION ^{14}C(^{11}B, ^{12}C)^{13}B AT E_{lab}(^{11}B) = 45 MeV, INTERACTION OF ^{13}B + ^{12}C VERSUS THAT OF ^{10,11,12}B + ^{12}C

New experimental data for differential cross-sections of the ^{14}C(^{11}B, ^{12}C)^{13}B reaction obtained recently at the energy E_{lab}(^{11}B) = 45 MeV for the ground states of ^{13}B and ^{12}C were analyzed within the coupled reaction channels (CRC) method that included the ^{11}B + ^{14}C elastic scattering channel as well as channels for one- and two-step transfers of nucleons in the coupling scheme. The necessary ^{11}B + ^{14}C Woods - Saxon (WS) optical potential parameters for the entrance reaction channel were obtained from ^{11}B elastic scattering in the previous work, while those for ^{12}C + ^{13}B interaction were deduced from fitting the CRC calculations to the ^{14}C(^{11}B, ^{12}C)^{13}B reaction data. Needed spectroscopic amplitudes of transferred nucleons and clusters were calculated within the translational-invariant shell model. The data are well described by the direct transfer of a proton while contributions from two-step transfers were found to be negligible. The deduced ^{13}B + ^{12}C WS optical potential parameters are compared with those of the ^{10,11,12}B + ^{12}C nuclei interactions. The effect of isotopic differences in these interactions was observed.

Keywords: nuclear reaction ^{14}C(^{11}B, ^{12}C)^{13}B, coupled-reaction-channels method, spectroscopic amplitudes, optical potentials, reaction mechanisms.

1. Introduction

For the study of the nuclear structure of boron isotopes and properties of their interaction with other nuclei, a lot of experimental and theoretical work has been performed up to date, with the use of stable ^{10,11}B isotopes serving as projectiles or targets in many direct experiments, as much fewer experiments have been performed with secondary $^{8,12-17}$B beams, thus the properties of unstable boron isotopes were investigated mainly through reactions in which they were produced as outgoing or residual nuclei. In particular, secondary beams of ^{13}B and other unstable boron isotopes were used in [1] with the aim to determine the radii of proton point distributions in $^{12-17}$B. Concerning the structure of ^{13}B, it was investigated in several indirect experiments such as [2] to probe the spectroscopy of $^{13-16}$B using multi-nucleon transfer reactions, or in [3] via the ^{12}B(d, p)^{13}B and in [4] via the ^{15}C(d, α)^{13}B reactions performed in inverse kinematics, as well as in [5] by the use of the reaction ^{13}C(t, ^{3}He)^{13}B. In [6], spectroscopic information about the final states of ^{13}B and ^{14}B was obtained from the reactions ^{14,15}C(d, ^{3}He)^{13,14}B also performed in inverse kinematics. In [7], the (d, p) reaction was used to determine the ^{11,12}B(n, γ) reaction rates and their influence on r-process nucleosynthesis for different astrophysical implications.

In this work, we continue the investigation of reaction ^{14}C(^{11}B, ^{12}C)^{13}B at E_{lab}(^{11}B) = 45 MeV with the main purpose as to deduce the Woods - Saxon (WS) potential for the final state interaction of ^{13}B + ^{12}C nuclei produced in the exit reaction channel, as well to compare it (study the *isotopic differences*) with the respective WS potentials deduced previously for the ^{12}B + ^{12}C [8], ^{11}B + ^{12}C [9] and ^{10}B + ^{12}C [10] interacting systems. As our recent publication [11] was focused on the study of spectroscopic properties of the interacting nuclei in this reaction ^{14}C(^{11}B, ^{12}C)^{13}B at E_{lab}(^{11}B) = 45 MeV, namely the extraction of the asymptotic normalization coefficient (ANC) for the ^{14}C → ^{13}B + p overlap, so the experimental part was presented very briefly as well as the interaction potentials, used for the best-fit coupled reaction channels (CRC) calculations, were not compared with the respective interaction potentials of other neighbouring nuclei. Thus, in this paper, we provide some more details and discussion regarding the above-mentioned issues. Finally, a test of the recently published global optical model (OM) potential for ^{8,10,11}B projectiles [12] is performed by its application to describe the interaction of ^{12}C + ^{13}B nuclei in the exit channel of the reaction ^{14}C(^{11}B, ^{12}C)^{13}B, as, at least, predicted matter radii of ^{10}B and ^{13}B differ by less than 0.1 fm

[13], so this potential with modifications proposed in [14] is used directly for the entrance $^{11}B + ^{14}C$ reaction channel and tested, with or without any modifications, for the exit $^{13}B + ^{12}C$ reaction channel.

2. Experimental procedure

Angular distributions of the $^{14}C(^{11}B, X)$ scattering and transfer reactions were measured simultaneously at an energy $E_{lab}(^{11}B)$ = 45 MeV using the ^{11}B beam from the Warsaw University cyclotron U-200P. A self-supporting 280 μg/cm^2 foil with 86 % enrichment by ^{14}C was used as a target. The experimental system has been described in [15, 16], so will not be repeated here, while a typical two-dimensional $\Delta E(E)$ spectrum of the registered reaction products is shown in Fig. 1 of [16]. The detailed energy spectrum of carbon isotopes is shown in the lower panel of Fig. 1 in [17]. In order to extract the peak areas necessary to obtain angular distributions of the reaction $^{14}C(^{11}B, ^{12}C)^{13}B$, firstly, a background function was constructed (code PEAKFIT) and fitted to the local minima of a given spectrum (Fig. 1, *a*) to account for maximum possible contributions of multi-particle reaction products. After subtraction of this smooth background, contributions from impurities in the target of the $^{12}C(^{11}B, ^{12}C)^{11}B$ reaction products in the ground and excited states, labeled in Fig. 1, *a*, *b*) as "$^{12}C)^{11}B$", were estimated using the spectra from $^{12}C + ^{11}B$ elastic and inelastic scattering measured at a slightly higher energy of $E_{lab}(^{11}B)$ = = 49 MeV [9] on the same experimental setup (solid curve in Fig. 1, *b*). After the subtraction of this background caused by ^{12}C impurities in the target, the obtained residual spectra (Fig. 1, *c*) were fitted with the sum of symmetric Gaussian functions with peak positions fixed at the energies predicted from kinematics. The same procedure as in [8] was used to minimize the contributions from residual backgrounds observed in the energy spectra. The maximum errors of the peak areas were estimated to be 30 %. The peaks corresponding to the reaction products $^{14}C(^{11}B, ^{12}C)^{13}B_{g.s.}$ were kinematically resolved from the peaks of the reaction $^{14}C(^{11}B, ^{14}C)^{11}B_{4.44}$ at $\Theta_{lab} > 17°$ and from $^{14}C(^{11}B, ^{14}C)^{11}B_{2.12}$ peaks at $\Theta_{lab} < 37°$. Peaks for the excited states of ^{13}B were obscured in carbon spectra by the strong peaks corresponding to excited ^{14}C or ^{11}B kinematically close to those of ^{13}B.

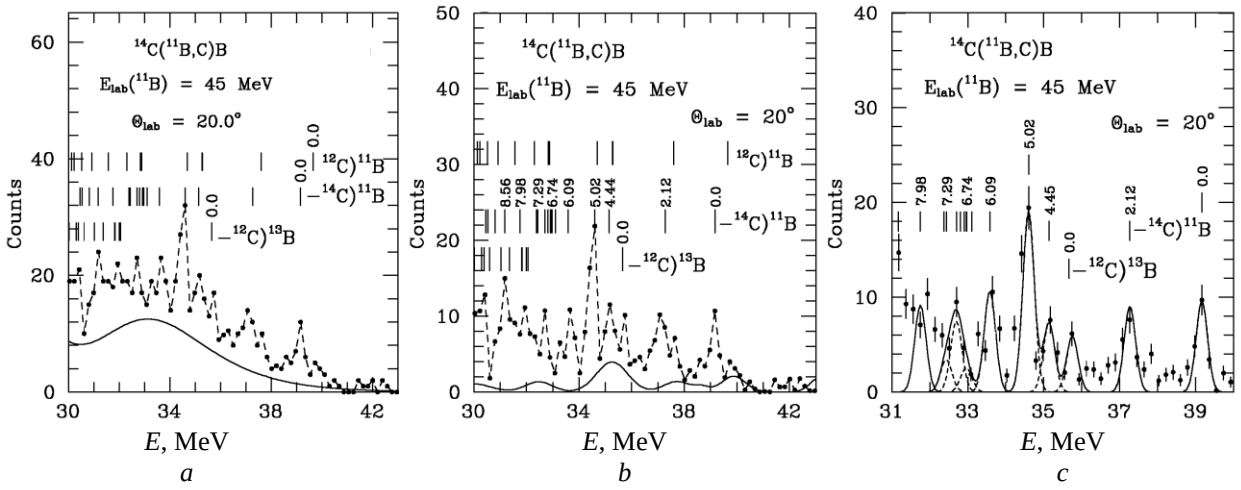

Fig. 1. Typical energy spectra of carbon isotopes from the $^{14}C(^{11}B, C)B$ reaction at the energy $E_{lab}(^{11}B)$ = 45 MeV. Curves show background forms of multi-particle reaction product contributions (*a*) and from ^{12}C impurities in the target (*b*), as well as Gauss symmetric fitted forms (*c*).

In this way, angular distributions of the reaction $^{14}C(^{11}B, ^{12}C)^{13}B_{g.s.}$ were obtained at the angles $\Theta_{c.m.}(^{12}C)$ only, as peaks of ^{13}B in the boron energy spectra were obscured by strong peaks of ^{11}B from the inelastic $^{11}B + ^{14}C$ scattering, thus making it not possible to derive any cross-sections for the angular distributions at $\Theta_{c.m.}(^{12}C) = 180^{\circ\theta} - \Theta_{c.m.}(^{13}B)$. The normalization factor, necessary to obtain the absolute cross-section of the $^{14}C(^{11}B, ^{12}C)^{13}B$ reaction, was the same as that used in the previous work of the elastic and inelastic scattering of ^{11}B by ^{14}C [16], measured in the same experiment.

3. Analysis of the reaction data

The $^{14}C(^{11}B, ^{12}C)^{13}B$ experimental data were analyzed within the CRC method. The $^{14}C + ^{11}B$ elastic scattering, including the reorientation of the ^{11}B [16], as well as transfer reactions as shown by diagrams in Fig. 2, were included in the channel coupling scheme. Standard WS optical potentials were used in the entrance and exit channels of the calculations and their form, given here for completeness, is:

$$U(r) = V_0\left[1+\exp\left(\frac{r-R_V}{a_V}\right)\right]^{-1} + \\ + iW_V\left[1+\exp\left(\frac{r-R_W}{a_W}\right)\right]^{-1} \quad (1)$$

with the Coulomb potential being that for uniformly charged spheres

$$V_C(r) = \begin{cases} Z_P Z_T e^2 (3 - r^2/R_C^2)/2R_C, & r \le R_C, \\ Z_P Z_T e^2 / r, & r > R_C. \end{cases} \quad (2)$$

Here, the form of the radii is given by:

$$R_i = r_i\left(A_P^{1/3} + A_T^{1/3}\right) \ (i = V, W, C), \quad (3)$$

where A_P, A_T and Z_P, Z_T are the mass and charge numbers of ^{11}B, ^{14}C (entrance channel), and ^{12}C, ^{13}B (exit channel). The parameter r_C = 1.25 fm was used in all CRC calculations.

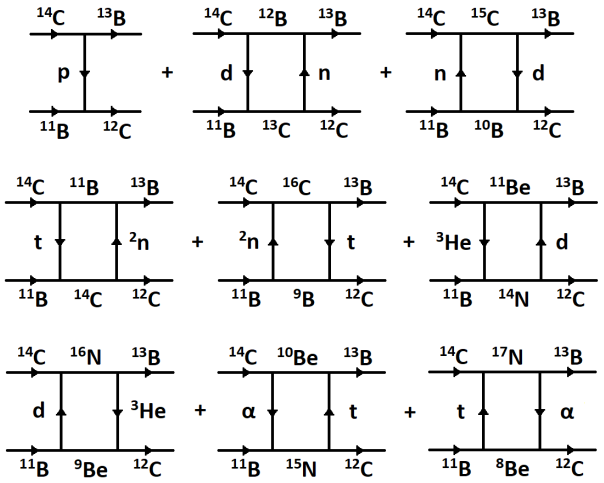

Fig. 2. Diagrams of different ^{14}C(^{11}B, ^{12}C)^{13}B reaction mechanisms.

The wave function of x for a nucleus $A = C + x$ was calculated by varying the depth of the WS binding potential to reproduce the binding energy of nucleus A. The geometry parameters of the cluster binding potentials were the following: a = 0.65 fm and $r_0 = 1.25\,A^{1/3}/(C^{1/3} + x^{1/3})$ fm.

The spectroscopic amplitudes S_x of clusters x for the nuclear systems $A = C + x$, used in the CRC calculations for the transfer reactions were obtained within the translational-invariant shell model (TISM) [18] using the computer code DESNA [19, 20] and Boyarkina's wave function tables for 1p-shell nuclei [21]. The calculated values of the amplitudes S_x are listed in Table 1.

The CRC calculations for the reaction ^{14}C(^{11}B, ^{12}C)^{13}B were performed with the code FRESCO [22]. For the entrance ^{11}B + ^{14}C channel the WS potential parameters were taken from [16], in which the elastic and inelastic scattering of these nuclei was investigated. The parameters of the WS potential for the ^{13}B + ^{12}C interaction were deduced from fitting the calculated cross-sections to the ^{14}C(^{11}B, ^{12}C)^{13}B experimental data, and they are listed in Table 2.

Angular distributions of the reaction ^{14}C(^{11}B, ^{12}C)^{13}B at E_{lab}(^{11}B) = 45 MeV for the ground states of ^{12}C and ^{13}B are shown in Fig. 3 together with CRC calculations for different transfer reactions. As can be seen, the direct transfer of a proton (curve <p>) is dominating in this reaction, while contributions of other two-step transfer reactions as d + n and n + d (curve <dn>, coherent sum), t + ^{2}n and ^{2}n + t (curve <t^{2}n>), d + ^{3}He and ^{3}He + d (curve <d^{3}He>), α + t and t + α (curve <αt>), are negligible.

Table 1. **Spectroscopic amplitudes S_x of x-clusters in the $A = C + x$ system**

A	C	x	nL_J	S_x	A	C	x	nL_J	S_x
^{11}B	^{8}Be	t	$2P_{3/2}$	0.641	^{14}C	^{10}Be	α	$3S_0$	–0.566
^{11}B	^{9}Be	d	$2S_1$	–0.607[a]	^{14}C	^{11}Be	^{3}He	$2S_{1/2}$	–0.903[a]
			$1D_1$	–0.109[a]	^{14}C	^{11}B	t	$2P_{3/2}$	–0.368[a]
			$1D_3$	0.610[a]	^{14}C	^{12}B	d	$1D_1$	–1.010
^{11}B	^{9}B	^{2}n	$2S_0$	–0.665	^{14}C	^{12}C	^{2}n	$2S_0$	0.615
			$1D_2$	0.421	^{14}C	^{13}B	p	$1P_{3/2}$	1.695[a]
^{11}B	^{10}B	n	$1P_{3/2}$	–1.347[a]	^{15}C	^{13}B	d	$2P_1$	–0.144
^{13}B	^{10}Be	t	$2P_{3/2}$	0.466				$1F_2$	–0.338[a]
^{13}B	^{11}Be	d	$2P_1$	–0.440	^{15}C	^{14}C	n	$2S_{1/2}$	–0.882
			$1F_1$	0.172	^{16}C	^{13}B	t	$3P_{3/2}$	0.342[a]
			$1F_2$	–0.517[a]	^{16}C	^{14}C	^{2}n	$3S_0$	–1.089
^{13}B	^{11}B	^{2}n	$2S_0$	0.623	^{14}N	^{11}B	^{3}He	$2P_{1/2}$	–0.107[a]
			$1D_2$	0.197				$2P_{3/2}$	–0.096
^{13}B	^{12}B	n	$1P_{1/2}$	–0.238				$1F_{5/2}$	–0.292[a]

Continuation of Table 1

A	C	x	nL_J	S_x		A	C	x	nL_J	S_x
			$1P_{3/2}$	0.213[a]		^{14}N	^{12}C	d	$1D_1$	0.246
^{12}C	^{8}Be	α	$3S_0$	0.822		^{15}N	^{11}B	α	$2D_2$	0.435[a]
^{12}C	^{9}Be	^{3}He	$2P_{3/2}$	1.224[a]		^{15}N	^{12}C	t	$2P_{1/2}$	0.380
^{12}C	^{9}B	t	$2P_{3/2}$	–1.224[a]		^{16}N	^{13}B	^{3}He	$3S_{1/2}$	–0.103
^{12}C	^{10}B	d	$1D_3$	1.780					$2D_{5/2}$	–0.140
^{12}C	^{11}B	p	$1P_{3/2}$	–1.706[a]					$1G_{7/2}$	0.137[a]
^{13}C	^{11}B	d	$2S_1$	–0.263		^{16}N	^{14}C	d	$2P_2$	0.380
			$1D_1$	–0.162		^{17}N	^{13}B	α	$3D_2$	–0.398[a]
			$1D_2$	–0.485[a]		^{17}N	^{14}C	t	$3P_{1/2}$	–0.817
^{13}C	^{12}C	n	$1P_{1/2}$	0.601						

[a] $S_{FRESCO} = (-1)^{J_C+j-J_A} \cdot S_x = -S_x$.

Table 2. **Parameters of optical potentials**

$T + P$	$E_{c.m.}$, MeV	V_0, MeV	r_V, fm	a_V, fm	W_S, MeV	r_W, fm	a_W, fm	Ref.
^{14}C + ^{11}B	25.20	266.6	0.750	0.740	7.5	1.345	0.740	[16]
^{12}C + ^{13}B	20.33	221.0	0.798	0.690	9.7	1.250	0.660	this work
^{12}C + ^{12}B	22.80	177.0	0.788	0.740	9.0	1.000	0.600	[8]
^{12}C + ^{11}B	20.87	252.0	0.788	0.670	7.4	1.250	0.670	[9]
^{12}C + ^{10}B	22.53	100.0	1.150	0.428	15.0	1.300	0.248	[10]

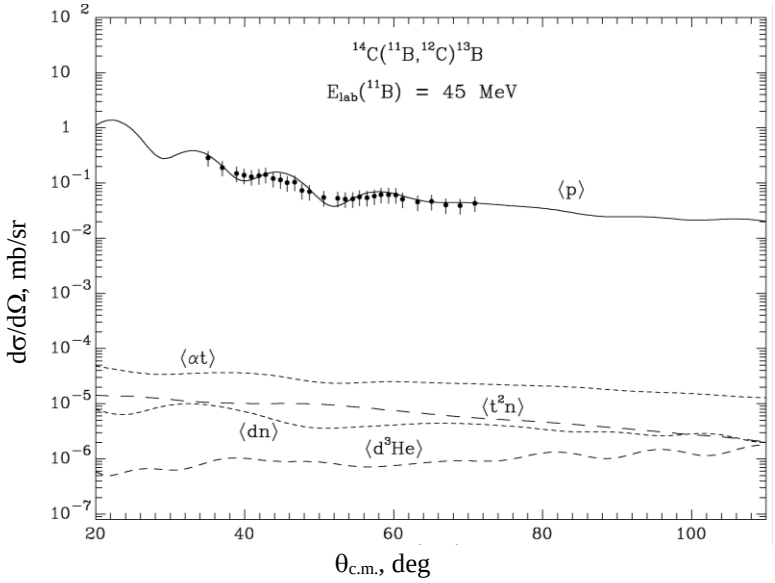

Fig. 3. Angular distribution of the ^{14}C(^{11}B, ^{12}C)^{13}B reaction at the energy E_{lab}(^{11}B) = 45 MeV for the ground states of ^{13}B and ^{12}C. The curves show CRC cross-sections calculated with the WS potentials (see Table 2) for different transfer processes.

In Fig. 4 the comparison of cross-sections for the direct transfer of a proton in the reaction ^{14}C(^{11}B, ^{12}C)^{13}B, calculated with OM parameters from this work for the ^{12}C + ^{13}B interaction, and the parameters used in the exit reaction channel as deduced previously for ^{12}C + ^{10}B [10], ^{12}C + ^{11}B [9] and ^{12}C + ^{12}B [8] interactions (see Table 2), are shown. The observed differences in the calculated cross-sections (so-called *isotopic effects*) may be caused, on one hand, by the different internal structures of $^{10\text{-}13}$B isotopes: the predicted matter radii [13] for ^{12}B and ^{13}B are equal (2.41 ± 0.03 and 2.41 ± 0.05 fm, respectively), a bit smaller for ^{10}B (2.34 ± 0.06 fm) and the smallest for ^{11}B (2.23 ± 0.11 fm), also the shapes for density distributions of neutrons (as well as matter) in $^{10\text{-}13}$B isotopes are predicted [13] to be different. The calculations in Fig. 4 with the use of WS potentials in the exit channel of the reaction ^{14}C(^{11}B, ^{12}C)^{13}B as deduced for ^{12}C + ^{10}B [10] and ^{12}C + ^{13}B (this work) interactions generate almost similar results at forwarding angles, but the difference is observed when the WS potential for ^{12}C + ^{12}B [8] interaction is used, and especially for ^{12}C + ^{11}B [9] interaction. The WS potentials for ^{12}C + ^{13}B (this work) and ^{12}C + ^{11}B [9] interactions differ mainly by the depths of the real and imaginary parts (see Table 2), and these differences of the potential well depths cause very different results of calculations as shown in Fig. 4 when potentials for ^{13}B + ^{12}C and ^{11}B + ^{12}C [9]

interactions are used in the exit channel of the reaction $^{14}C(^{11}B, ^{12}C)^{13}B$. The choice of the individual parameters of WS potential for a given interaction system, on the other hand, is connected with the important channel couplings taken into account in the analysis of experimental data: for example for the $^{11}B + ^{12}C$ elastic scattering the inclusion of proton transfer between the projectile and the target and transition to the first 4.445 MeV (2^+) excited state of ^{12}C were shown to have a significant effect on the results of calculations [23], both of these processes were taken into account in the analysis of $^{12}C + ^{11}B$ elastic scattering data in a broad energy range [9].

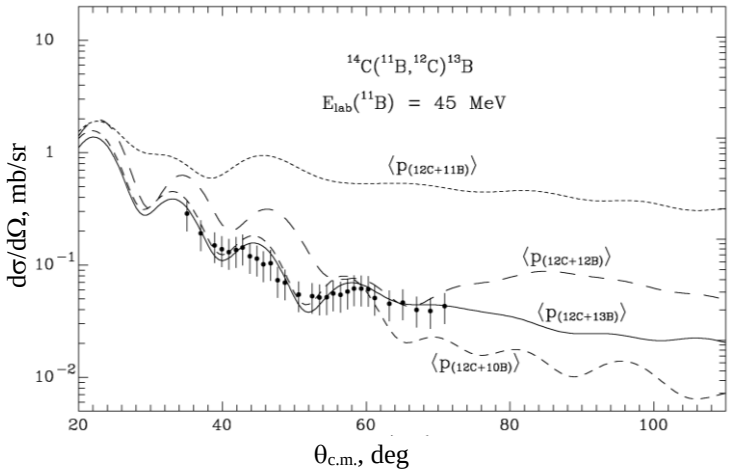

Fig. 4. Angular distributions of the $^{14}C(^{11}B, ^{12}C)^{13}B$ reaction for the ground states of ^{13}B and ^{12}C. The curves show CRC calculations for proton transfer with different OM parameters for the $^{13}B + ^{12}C$ interaction (see Table 2).

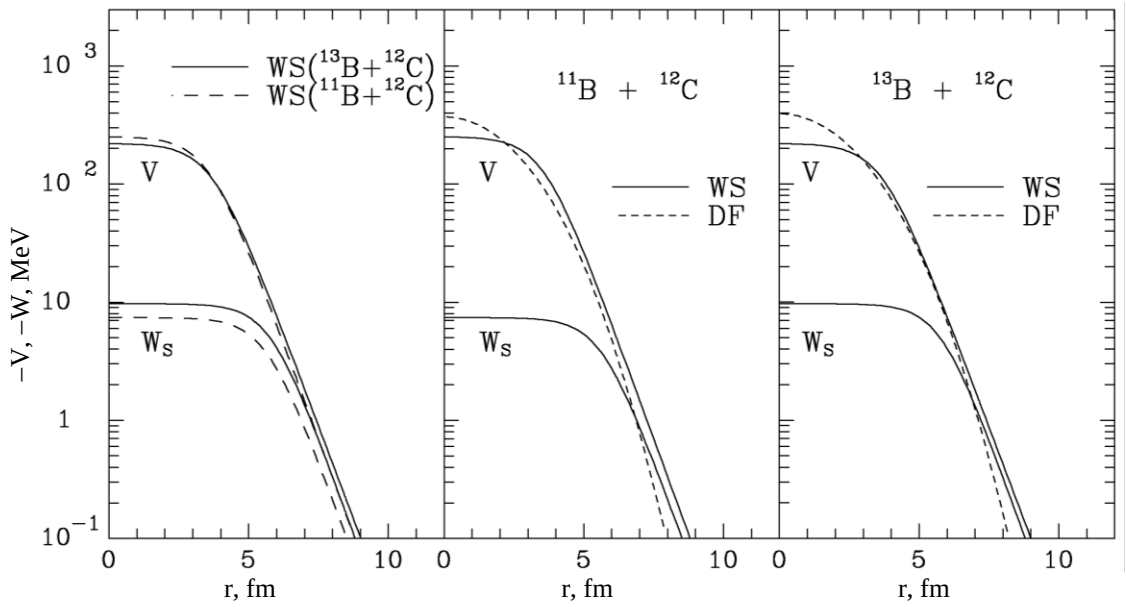

Fig. 5. The radial dependence of the volume real and imaginary parts of WS potentials for $^{13}B + ^{12}C$ and $^{11}B + ^{12}C$ interactions from Table 2 (*left-hand side*), WS and DF potentials for $^{11}B + ^{12}C$ (*middle*), and $^{13}B + ^{12}C$ (*right-hand side*) interactions. See captions in the Figure and text for details.

In the left-hand side of Fig. 5, the radial dependence of the volume real (V_0) and imaginary (W_S) parts of WS potentials (see Table 2) for $^{11}B + ^{12}C$ and $^{13}B + ^{12}C$ interaction is shown. In an attempt to find some possible connection of the observed difference of the real parts of these potentials with the internal structure of ^{11}B and ^{13}B isotopes, we used the shapes for the density distributions of protons and neutrons in ^{11}B, ^{13}B, and ^{12}C predicted in [13] and M3Y Reid form of nucleon-nucleon interaction [24], to generate folding-model (DF) potentials for $^{11}B + ^{12}C$ and $^{13}B + ^{12}C$ interaction systems using code DFPOT [25]. In the middle of Fig. 5, the comparison of the WS [9] and DF potentials for the $^{11}B + ^{12}C$ system is shown, as can be seen, the deduced WS potential [9] is somewhat broader than the generated DF potential. In the right-hand side of Fig. 5, the same potentials are shown for the $^{13}B + ^{12}C$ system, and an excellent agreement in the interaction region (5 - 7 fm) between the real parts of WS and DF potentials is observed. It is interesting to compare the results of CRC fit to the $^{12}C + ^{11}B$ [9], $^{12}C + ^{10}B$ [10] elastic scattering data, as well as the reactions

^{13}C(^{11}B, ^{12}C)^{12}B [8] and ^{14}C(^{11}B, ^{12}C)^{13}B (this work) with the use of previously deduced WS potentials and the DF potentials generated for ^{10,11,12,13}B + ^{12}C systems using the predicted shapes for the density distributions of protons and neutrons in these nuclei [13], what will be done by us in the future.

Finally, we performed test calculations for the transfer of a proton in the reaction ^{14}C(^{11}B, ^{12}C)^{13}B at E_{lab}(^{11}B) = 45 MeV using the parameters of global OM potential for ^{8,10,11}B projectiles proposed in [12]. The parameters of the real volume (V_0, r_V, a_V), imaginary volume (W_S, r_W, a_W), and imaginary surface (W_D, r_D, a_D) parts of WS OM potentials for ^{14}C + ^{11}B and ^{12}C + ^{13}B interactions were generated from global systematics [12] and are listed in Table 3, for Coulomb interaction $V_C(r)$ (2) the parameter r_C = 1.556 fm was used for both reaction channels. It should be noted that the radii of these potentials are dependent on the target masses only as $R_i = r_i A_T^{1/3}$ (i = V, W, D, C). The detailed expressions of these potentials can be found also in [8, 14].

Table 3. **Parameters of the global OM potentials from Ref. [12] original (a), (c) and modified (b), (d)**

$T + P$	V_0, MeV	r_V, fm	a_V, fm	W_S, MeV	r_W, fm	a_W, fm	W_D, MeV	r_D, fm	a_D, fm	Potentials
^{14}C + ^{11}B	258.14	1.266	0.726	15.84	1.640	0.600	45.52	1.200	0.843	(a)
^{14}C + ^{11}B	258.14	1.566	0.726	13.34	1.940	0.900				(b)
^{12}C + ^{13}B	258.83	1.263	0.726	15.08	1.640	0.600	46.86	1.200	0.843	(c)
^{12}C + ^{13}B	258.83	1.263	0.726	15.08	1.940	0.800				(d)

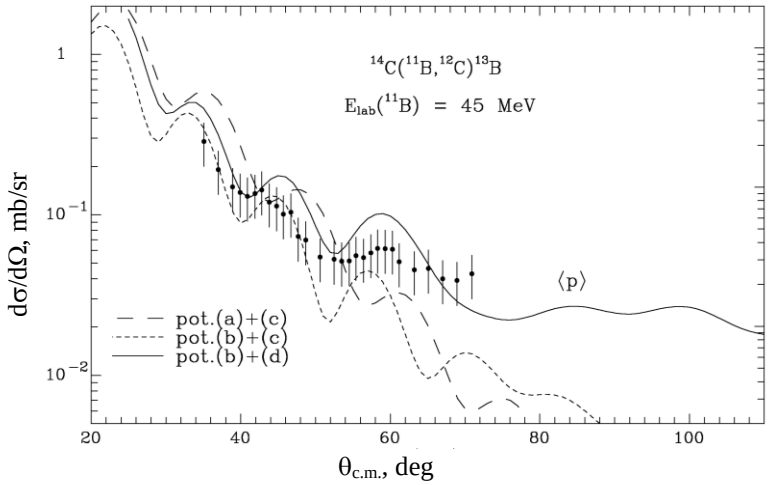

Fig. 6. Angular distributions of the ^{14}C(^{11}B, ^{12}C)^{13}B reaction for the ground states of ^{13}B and ^{12}C. The curves show CRC cross-sections for the transfer of a proton, calculated with different parameters of OM potentials from Table 3 (see text and captions in the Figure for details).

The results of calculations of a proton transfer in the reaction ^{14}C(^{11}B, ^{12}C)^{13}B with the use of original OM potential parameters generated from global systematics [12] for the entrance (potential (a)) and exit (potential (c)) reaction channels are shown in Fig. 6 by the long-dashed curve, which, as can be seen, is not in a good agreement with the experimental data. Because for the elastic ^{11}B + ^{14}C scattering at E_{lab}(^{11}B) = 45 MeV calculations with original potential parameters (potential (a)) strongly underestimated the experimental data at backward angles and diffraction phase disagreement was also observed at forwarding angles [14], some modifications of this potential were proposed (potential (b)) in order to reach a much better agreement with both forward and backward angle experimental data for the ^{11}B + ^{14}C elastic scattering [14]. So, using the modified OM potential (potential (b)) for the entrance channel of the rection ^{14}C(^{11}B, ^{12}C)^{13}B but leaving the original (potential (c)) potential for the exit channel leads to the improvement of the data fit only for $\Theta_{c.m.} < 50°$ as shown in Fig. 6 by the short-dashed curve. As was shown in [14] from the analysis of the ^{14}C(^{11}B, ^{10}B)^{15}C reaction data, strong absorption caused by the imaginary surface potential [12] leads to the calculated cross-sections being lower than the experimental data. Thus, using the same procedure as in [14], e.g., omitting the surface term of the global OM potential for ^{13}B + ^{12}C interaction and slightly changing the parameters of the volume terms (potential (d)), we could get a somewhat better agreement with the experimental data (solid curve in Fig. 6).

4. Summary and conclusions

New experimental data for differential cross-sections of the reaction ^{14}C(^{11}B, ^{12}C)^{13}B at E_{lab}(^{11}B) = 45 MeV obtained in the forward angle hemisphere for the ground states of ^{13}B and ^{12}C and published recently in [11], were analyzed within the CRC method that included the elastic and inelastic scattering channels of ^{11}B + ^{14}C as well as one- and two-step transfers in the coupling scheme.

For the entrance reaction channel, a WS potential was used with the parameters deduced from a previous CRC analysis of the experimental data for ^{11}B + ^{14}C elastic scattering at E_{lab}(^{11}B) = 45 MeV [16]. Spectroscopic amplitudes for nucleons and clusters, needed for the CRC calculations of the reaction cross-sections, were obtained within the TISM [18] by means of the computer code DESNA [20]. The spectroscopic *factors* of nucleons and clusters in nuclei are defined by the squares of these spectroscopic amplitudes. The parameters of WS potential for the ^{13}B + ^{12}C interaction were deduced from the fit of CRC cross-sections to the ^{14}C(^{11}B, ^{12}C)^{13}B reaction data.

From the present CRC analysis of the experimental data for the reaction ^{14}C(^{11}B, ^{12}C)^{13}B it was found that direct transfer of a proton is dominating, while contributions of two-step transfers of nucleons and clusters are negligible.

Comparison of the parameters of WS potentials for the interaction of ^{12}C + ^{13}B, ^{12}C + ^{10}B [10], ^{12}C + ^{11}B [9], and ^{12}C + ^{12}B [8] as well as CRC cross-sections for the reaction ^{14}C(^{11}B, ^{12}C)^{13}B with the use of these potentials for the exit reaction channel, was performed. Differences in these cross-sections were observed that might be due to different internal structures, for instance, different shapes of matter distributions in $^{10\text{-}13}$B isotopes as predicted in [13], as well as some important channel-coupling effects taken into account in the analysis of experimental data, for given interaction systems.

Global OM potential proposed for ^{8,10,11}B projectiles [12] was tested as part of the analysis for the system ^{13}B + ^{12}C and CRC calculations with OM parameters extracted from global systematics [12] were found to reproduce the experimental data of the reaction ^{14}C(^{11}B, ^{12}C)^{13}B at E_{lab}(^{11}B) = 45 MeV only when surface terms of this potential were omitted for both reaction channels, as well as the parameters of the volume real and imaginary potentials, were slightly modified, similar to what had been derived recently from the analysis of the ^{14}C(^{11}B, ^{10}B)^{15}C reaction data [14]. For the further test of the applicability of global OM potential [12] to ^{13}B projectiles, the measurements of experimental data for ^{13}B scattering from light and heavy targets is desirable, with special attention to be paid to other inelastic processes, besides pure potential scattering, in the analysis of experimental data of ^{13}B elastic scattering from light targets [12, 14].

The Ukrainian authors from the Institute for Nuclear Research thank the co-authors from Polish and American scientific facilities for their moral support and readiness to provide any help, due to the invasion of russian armed forces on the territory of Ukraine from the 24th of February 2022. We also thank them for solidarity in condemnation of this military aggression and are full of hope that soon this war horror will come to an end for good.

REFERENCES

1. A. Estradé et al. Proton Radii of $^{12\text{-}17}$B Define a Thick Neutron Surface in ^{17}B. Phys. Rev. Lett. 113 (2014) 132501.
2. R. Kalpakchieva et al. Spectroscopy of ^{13}B, ^{14}B, ^{15}B and ^{16}B using multi-nucleon transfer reactions. Eur. Phys. J. A 7 (2000) 451.
3. B.B. Back et al. First Experiment with HELIOS: The Structure of ^{13}B. Phys. Rev. Lett. 104(13) (2010) 132501.
4. A.H. Wuosmaa et al. Stretched states in ^{12,13}B with the (d, α) reaction. Phys. Rev. C 90 (2014) 061301.
5. C.J. Guess et al. Spectroscopy of ^{13}B via the ^{13}C(t, ^{3}He) reaction at 115A MeV. Phys. Rev. C 80 (2009) 024305.
6. S. Bedoor et al. Structure of ^{14}C and ^{14}B from the ^{14,15}C(d, ^{3}He)^{13,14}B reactions. Phys. Rev. C 93(4) (2016) 044323.
7. H.Y. Lee et al. Experimental study of the ^{11,12}B(n, γ) reactions and their influence on r-process nucleosynthesis of light elements. Phys. Rev. C 81 (2010) 015802.
8. S.Yu. Mezhevych et al. ^{13}C(^{11}B, ^{12}C)^{12}B reaction at 45 MeV, ^{12}C + ^{12}B interaction versus that of ^{12}C + + ^{10,11}B. Acta Phys. Pol. B 51(10) (2020) 1949.
9. A.T. Rudchik et al. The ^{11}B + ^{12}C elastic and inelastic scattering at E_{lab}(^{11}B) = 49 MeV and energy dependence of the ^{11}B + ^{12}C interaction. Nucl. Phys. A 695 (2001) 51.
10. N. Burtebayev et al. Measurement and analysis of ^{10}B + ^{12}C elastic scattering at energy of 41.3 MeV. Int. J. Mod. Phys. E 28 (2019) 1950028.
11. S.Yu. Mezhevych et al. Extracting the asymptotic normalization coefficient for the ^{14}C → ^{13}B + p overlap from the ^{14}C(^{11}B, ^{12}C)^{13}B reaction. Phys. Rev. C 105 (2022) 024615.
12. Yong-Li Xu et al. Applicability of ^{9}Be global optical potential to description of ^{8,10,11}B elastic scattering. Chinese Physics C 44(3) (2020) 034101.
13. Suhel Ahmad, A.A. Usmani, Z.A. Khan. Matter radii of light proton-rich and neutron-rich nuclear isotopes. Phys. Rev. C 96 (2017) 064602.
14. S.Yu. Mezhevych et al. Reaction ^{14}C(^{11}B, ^{10}B)^{15}C at E_{lab} = 45 MeV and ^{10}B + ^{15}C optical potential. Acta Phys. Pol. B 52(2) (2021) 109.
15. S.Yu. Mezhevych et al. The ^{13}C + ^{11}B elastic and inelastic scattering and isotopic effects in the ^{12,13}C + ^{11}B scattering. Nucl. Phys. A 724(1-2) (2003) 29.
16. S.Yu. Mezhevych et al. Elastic and inelastic scattering of ^{14}C + ^{11}B versus ^{12,13}C + ^{11}B. Eur. Phys. J. A 50 (2014) 4.
17. S.Yu. Mezhevych et al. Excitation of ^{14}C by 45 MeV ^{11}B ions. Nucl. Phys. A 753 (2005) 13.

18. Yu.F. Smirnov, Yu.M. Tchuvil'sky. Cluster spectroscopic factors for the *p*-shell nuclei. Phys. Rev. C 15 (1977) 84.
19. A.T. Rudchik, Yu.M. Tchuvil'sky. Spectroscopic amplitudes of multinucleon clusters in 1p-shell nuclei and analysis of multinucleon transfer reactions. Ukrainian Journal of Physics 30(6) (1985) 819. (Rus)
20. A.T. Rudchik, Yu.M. Tchuvil'sky. Calculation of spectroscopic amplitudes for arbitrary associations of nucleus in 1p-shell nuclei (program DESNA). Prepr. of the Institute for Nucl. Res., AS UkrSSR. KINR-82-12 (Kyiv, 1982) 27 p. (Rus)
21. A.N. Boyarkina. *The Structure of the 1p-shell Nuclei* (Moskva: Moscow University, 1973) 62 p. (Rus)
22. I.J. Thompson. Coupled reaction channels calculations in nuclear physics. Comp. Phys. Rep. 7 (1988) 167.
23. S.Yu. Mezhevych, K. Rusek. Quadrupole deformation of ^{11}B (3/2$^-$, 5.02 MeV) excited state from ^{11}B + + ^{12}C scattering. Acta Phys. Pol. B 34(4) (2003) 2415.
24. G. Bertsch et al. Interactions for inelastic scattering derived from realistic potentials. Nucl. Phys. A 284(3) (1977) 399.
25. J. Cook. DFPOT – A program for the calculation of double folded potentials. Comput. Phys. Commun. 25 (1982) 125.

С. Ю. Межевич[1,*], А. Т. Рудчик[1], К. Русек[2], К. В. Кемпер[3], А. А. Рудчик[1], О. А. Понкратенко[1], Є. І. Кощий[4]

[1] Інститут ядерних досліджень НАН України, Київ, Україна
[2] Лабораторія важких іонів Варшавського університету, Варшава, Польща
[3] Відділ фізики Флоридського державного університету, Таллахассі, США
[4] Циклотронний інститут Техаського A&M університету, Колледж Стейшен, США

*Відповідальний автор: sermezhev@gmail.com

РЕАКЦІЯ ^{14}C(^{11}B, ^{12}C)^{13}B ПРИ ЕНЕРГІЇ $E_{лаб.}$(^{11}B) = 45 МеВ, ВЗАЄМОДІЯ ЯДЕР ^{13}B + ^{12}C ТА ^{10,11,12}B + ^{12}C

Нещодавно отримані нові експериментальні дані диференціальних перерізів реакції ^{14}C(^{11}B, ^{12}C)^{13}B при енергії $E_{лаб.}$(^{11}B) = 45 МеВ для основних станів ядер ^{13}B та ^{12}C проаналізовано за методом зв'язаних каналів реакцій (МЗКР), у схему зв'язку було включено канал пружного розсіяння ядер ^{11}B + ^{14}C та канали одно- й двоступінчастих передач нуклонів і кластерів. Для вхідного каналу реакції необхідні параметри оптичного потенціалу Вудса - Саксона було використано з аналізу пружного розсіяння ^{11}B з попередньої роботи, а параметри для взаємодії ^{12}C + ^{13}B було отримано з підгонки МЗКР-розрахунків до експериментальних даних реакції ^{14}C(^{11}B, ^{12}C)^{13}B. Необхідні спектроскопічні амплітуди (фактори) для переданих нуклонів і кластерів було обчислено за трансляційно-інваріантною моделлю оболонок. Дані добре описуються прямою передачею протона, а вклади двоступінчастих реакцій передач виявились незначними. Проведено порівняння параметрів потенціалу Вудса - Саксона, визначених для взаємодії ядер ^{13}B + ^{12}C, з параметрами цих потенціалів для систем ^{10,11,12}B + ^{12}C. Спостерігається ефект ізотопічної відмінності цих взаємодій.

Ключові слова: ядерна реакція ^{14}C(^{11}B, ^{12}C)^{13}B, метод зв'язаних каналів реакцій, спектроскопічні амплітуди, оптичні потенціали, механізми реакцій.

Надійшла/Received 23.11.2021